

Molecular Origin of Rapid versus Slow Intramolecular Electron Transfer in the Catalytic Cycle of the Multicopper Oxidases

David E. Heppner, Christian H. Kjaergaard, and Edward I. Solomon*

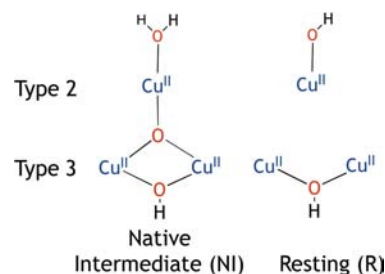
Department of Chemistry, Stanford University, Stanford, California 94305, United States

S Supporting Information

ABSTRACT: Kinetic measurements on single-turnover processes in laccase established fast type-1 Cu to trinuclear Cu cluster (TNC) intramolecular electron transfer (IET) in the reduction of the native intermediate (NI), the fully oxidized form of the enzyme formed immediately after O–O bond cleavage in the mechanism of O₂ reduction. Alternatively, slow IET kinetics was observed in the reduction of the resting enzyme, which involves proton-coupled electron transfer on the basis of isotope measurements. The >10³ difference between the IET rates for these two processes confirms that the NI, rather than the resting enzyme that has been defined by crystallography, is the fully oxidized form of the TNC in catalytic turnover. Computational modeling showed that reduction of NI is fast because of the larger driving force associated with a more favorable proton affinity of its μ₃-oxo moiety generated by reductive cleavage of the O–O bond. This defines a unifying mechanism in which reductive cleavage of the O–O bond is coupled to rapid IET in the multicopper oxidases.

Reduction of dioxygen to water is performed in nature by the multicopper oxidases (MCOs) to carry out a variety of single-electron oxidations of metal ion or organic substrates.^{1,2} This requires at least four Cu ions: a type-1 (T1)^{3,4} Cu site and a trinuclear Cu cluster (TNC)^{5,6} composed of mononuclear type-2 (T2) and coupled binuclear type-3 (T3) Cu centers. The T1 site receives electrons from the substrate and transfers them through the protein over ~13 Å to the TNC, where O₂ binds and is reduced. Understanding of the chemistry of these enzymes has been motivated by their relevance to human health (ceruloplasmin)⁷ and application to biofuel cells.^{8,9} The mechanism of O₂ reduction has been well-studied.² The fully reduced enzyme (4 Cu^I) reacts with O₂ to form the peroxy intermediate (2 Cu^I, 2 Cu^{II}), where O₂ is bound as peroxide to the TNC. This then undergoes O–O bond cleavage accompanied by protonation of one oxygen to produce the native intermediate (NI) (Scheme 1 left). In this intermediate, which is fully oxidized (4 Cu^{II}), all three Cu ions of the TNC are bridged by a μ₃-oxo and the T3 ions are additionally bridged by a μ₂-OH. Both moieties originate from the four-electron reduction of O₂.¹⁰ NI is structurally distinct from the fully oxidized resting form of the enzyme (R) that is observed crystallographically^{11,12} with respect to the bridging ligands, in that R has only the μ₂-OH bridge between the T3 Cu ions (Scheme 1 right).¹³

Scheme 1. Experimentally Determined Geometric Structures of the TNC in the NI and R States



While much effort has been devoted to describing the mechanism of O₂ reduction by the MCOs, the mechanism of rereduction in catalysis is less explored, especially concerning the rates of intramolecular electron transfer (IET) from the T1 site to the TNC. The most well-studied enzyme in the MCO family is *Rhus vernicifera* laccase (Lc), which naturally oxidizes phenolic substrates with a maximal turnover rate of 560 s⁻¹ at 25 °C.¹⁴ However, the IET rates for R measured using pulsed radiolysis (1.1 s⁻¹ at 25 °C) are low relative to this turnover rate, excluding the reduction of R from the catalytic cycle.¹⁵ Upon reaction with O₂, NI forms rapidly and decays slowly (0.058 s⁻¹ at 23 °C),¹⁶ which strongly suggests that NI is reduced directly with fast IET rates to be consistent with turnover.¹ For the first time, we report kinetic studies of the reduction of NI that demonstrate fast IET and thus the relevance of this intermediate in the reduction cycle in turnover. This is important because it demonstrates that NI, not R studied by crystallography (Scheme 1), is the fully oxidized form of the enzyme that is catalytically active. Parallel experiments on the slow IET in R have defined the geometric and electronic structural contributions of the TNC in NI that determine its fast IET.

Monitoring of the absorption spectral changes via the stopped-flow (SF) method in the reaction of fully reduced Lc (50 μM) with equimolar O₂ showed initial rapid (~10⁶ M⁻¹ s⁻¹) formation of NI on the basis of the appearance of its 365 nm band associated with the μ₃-oxo to Cu^{II}₃ charge transfer (CT) at the TNC and the 614 nm Cys to Cu^{II} CT of the oxidized T1 site.^{17,18} This was followed by slow first-order decay (0.0070 s⁻¹) of the 365 nm band while the T1 site remained oxidized, consistent with previous findings on the formation rate of NI and its decay to R [Figure S1 in the

Received: June 25, 2013

Published: July 31, 2013

Supporting Information (SI)]. Carrying out the same SF experiment with 5.0 electron equivalents of hydroquinone (H_2Q), a widely used phenolic substrate for kinetic studies of Lc,^{14,19} added to fully reduced Lc led to analogous NI formation followed by decay of both the 365 and 614 nm bands (Figure 1A). The 365 nm band (red in Figure 1A,B) decayed in

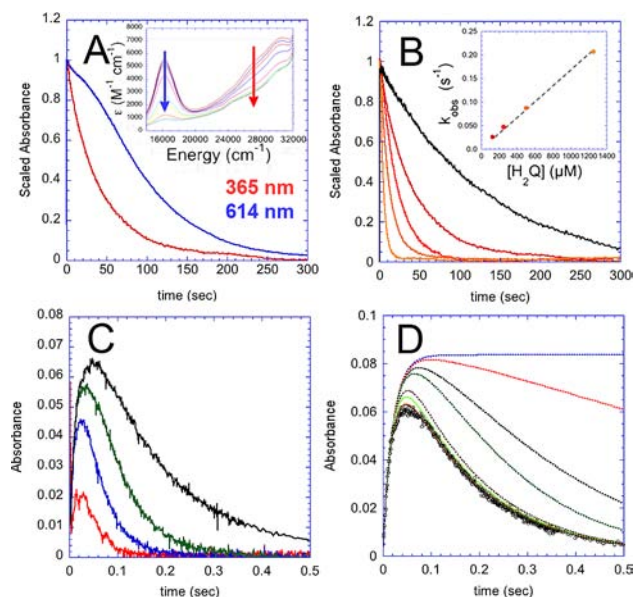


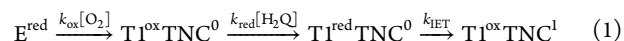
Figure 1. (A) Scaled absorption traces of the T1 (614 nm, blue) and TNC (365 nm, red) sites in the reduction of NI. Conditions: $[\text{Lc}] = [\text{O}_2] = 0.050 \text{ mM}$; $[\text{H}_2\text{Q}] = 0.125 \text{ mM}$. The inset shows time-dependent absorption spectra from 1 to 300 s. (B) $[\text{H}_2\text{Q}]$ dependence of the 365 nm trace (black, $[\text{H}_2\text{Q}] = 0.00 \text{ mM}$; red to orange, $[\text{H}_2\text{Q}] = 0.125, 0.250, 0.500, \text{ and } 1.25 \text{ mM}$). The inset shows the first-order dependence of the 365 nm decay on $[\text{H}_2\text{Q}]$. The colors of the traces match the colors of the dots in the inset. (C) Traces of the 365 nm band under conditions identical to those in (A) except with 42.8 (black), 85.5 (green), 145 (blue), and 271 (red) mM $[\text{H}_2\text{Q}]$. (D) Data from (C) with $[\text{H}_2\text{Q}] = 42.8 \text{ mM}$ and illustrative fits of these data using $k_{\text{IET}} = 0, 1, 5, 10, 50, 100, 500, \text{ and } 1000 \text{ s}^{-1}$.

a first-order fashion ($k = 0.029 \text{ s}^{-1}$), which was accelerated ~ 4 -fold over the rate of decay of NI (Figure 1B, black). Therefore, NI was reduced before it could decay with minimal excess substrate. The 365 nm decay rate increased linearly with $[\text{H}_2\text{Q}]$ (Figure 1B, red to orange), affording a second-order rate constant of $168.2 \text{ M}^{-1} \text{ s}^{-1}$ (Figure 1B inset).

Full reduction of the MCOs requires four electrons; H_2Q first reduces the T1 site, with subsequent IET to reduce the TNC. This occurs three times to fully reduce the TNC, with the fourth electron reducing the T1 site. The SF traces in Figure 1A indicate a number of points concerning the reduction of NI. The 614 nm band (Figure 1A, blue) decayed in a multiphasic fashion with limited loss of intensity at $t < 20 \text{ s}$, indicating that the T1 site effectively remains oxidized during the early stages of the reaction (Figure S3). Since electrons enter at the T1 Cu but no reduction of the T1 site (i.e., loss of intensity at 614 nm) was evident, the T1 reoxidation was rapid, indicating fast IET. This was further substantiated by the decay of the 365 nm band being first-order in $[\text{H}_2\text{Q}]$ (Figure 1B inset).

Since the absorption at 365 nm is due to the μ_3 -oxo to Cu^{II}_3 CT of NI,¹⁸ it is eliminated with the entry of the first electron into the TNC because this significantly alters the electronic

structure of NI. Therefore, the kinetics of this band intensity can provide a direct probe of the rate of the first IET in NI reduction, which can be fit to the mechanism shown in eq 1, which accounts for the formation of NI (denoted as $\text{T1}^{\text{ox}}\text{TNC}^0$, where the superscript of T1 indicates the oxidation state of the T1 site and the superscript of TNC shows the number of reduced Cu ions in the TNC) followed by H_2Q reduction of the T1 site and subsequent IET from the T1 site to the TNC. The species absorbing at 365 nm in this mechanism would be the two TNC^0 intermediates, since reduction of the T1 site does not alter the absorption at the TNC.



To obtain an estimate of k_{IET} , SF traces at 365 nm were obtained at higher $[\text{H}_2\text{Q}]$ (Figure 1C), where the T1 reduction rate was increased such that NI intensity was not maximized. Fits to the rate law derived from eq 1 were obtained with $k_{\text{ox}} = 1.2 \times 10^6 \text{ M}^{-1} \text{ s}^{-1}$, $k_{\text{red}} = 182.7 \text{ M}^{-1} \text{ s}^{-1}$, and $k_{\text{IET}} > 700 \text{ s}^{-1}$ (Figure S8). This value of k_{IET} is a lower limit, as illustrated in Figure 1D, where the fits of eq 1 to the high- $[\text{H}_2\text{Q}]$ data converge for $k_{\text{IET}} > 700 \text{ s}^{-1}$. This is significant because it establishes that IET in the MCOs for the reduction of NI is faster than turnover, while its decay is much slower (vide supra), and therefore requires that NI reduction is the catalytically relevant process for the rereduction of the fully oxidized enzyme.

As low IET rates in R have been reported with another method,¹⁵ parallel kinetic studies were conducted on R to obtain the rate difference under identical conditions. SF traces were obtained for the 330 nm band (μ_2 -OH to T3 Cu^{II}_2 CT) and the 614 nm band (T1 Cu^{II}) upon anaerobic reaction of R with H_2Q (Figure 2B). The 614 nm band trace was multiphasic

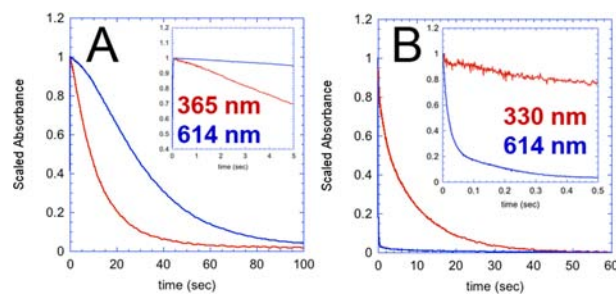


Figure 2. (A) Scaled absorption traces of the T1 (614 nm, blue) and TNC (365 nm, red) bands in the reduction of NI. Conditions: $[\text{Lc}] = [\text{O}_2] = 0.050 \text{ mM}$; $[\text{H}_2\text{Q}] = 0.500 \text{ mM}$. (B) Scaled absorption traces of the T1 (614 nm, blue) and TNC (330 nm, red) bands in the reduction of R. Conditions: $[\text{Lc}] = 0.050 \text{ mM}$; $[\text{H}_2\text{Q}] = 97.5 \text{ mM}$.

and decayed initially at a rate proportional to $[\text{H}_2\text{Q}]$, which is the opposite of the behavior observed in NI reduction, where the T1 site was mostly oxidized initially and the TNC reduction was proportional to $[\text{H}_2\text{Q}]$, implying slow IET in R (blue traces in Figure 2). The decay of the 330 nm band of R was first-order and invariant with respect to $[\text{H}_2\text{Q}]$ and exhibited biphasic behavior with a major component ($\sim 75\%$) having a rate constant of 0.111 s^{-1} and a minor ($\sim 25\%$) component having a rate constant of 1.29 s^{-1} (Figure S10). The slow decay of the 330 nm band for both components and its substrate independence demonstrate that IET from the T1 site to the TNC in R is slow relative to T1 reduction (and turnover).

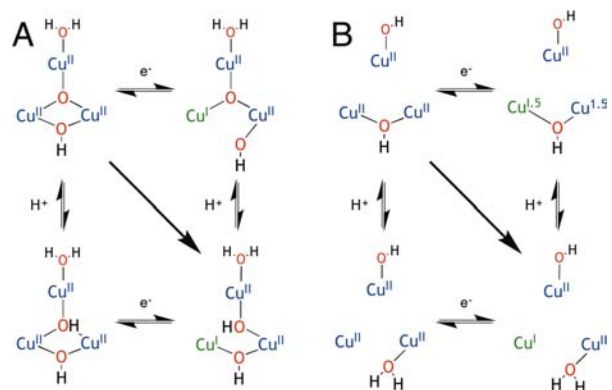
Kinetic experiments were performed at pH 6.5–8.5 (Figures S12–14). At high pH, the 614 nm band decayed faster,

consistent with the first pK_a of 9–10 for H_2Q .²⁰ Because of its limited contribution, the minor component of the 330 nm band reduction was difficult to study, while the rate of reduction of the major component clearly increased at low pH. The major component exhibited an inverse solvent kinetic isotope effect (SKIE) of 0.67 (Figure S11). This SKIE on the IET rate can be understood on the basis of the Westheimer model, where the bonds in the transition state are stronger than those in the reactant complex.²¹ Since the protons are delivered to the TNC via a distal carboxylate residue, these have a weaker O–H bond than the $Cu^{II}OH_2$ complex resulting from protonation of the T3 μ_2 -OH bridge (Scheme 2B).^{10,22} There could also be a secondary isotope effect from the substitutable proton on the oxygen of the T3 μ_2 -OH bridge (Figure S15).²³ Importantly, the observed SKIE on decay of the 330 nm absorption requires that a proton be involved in the IET in R. Thus, this is a proton-coupled electron transfer process (PCET). IET in NI at pH 7.5 is too fast for a measurement of the SKIE. However, since R has an SKIE that involves protonation of the T3 μ_2 -OH and NI has a μ_3 -oxo bridge that is more basic (vide infra), the IET in NI reduction must also involve a PCET process.

The observation of this $>10^3$ difference in IET rates ($>700\text{ s}^{-1}$ in NI, 0.111 s^{-1} in R) provides an opportunity to determine the molecular factor(s) that lead to fast IET in the MCOs. It can be assumed that electrons and protons come from sites (T1 and carboxylate, respectively) that do not vary much between NI and R. Therefore, the $>10^3$ difference in rates reflects the structures of the TNC electron and proton acceptors. In the context of Marcus theory, first-order IET rates can be expressed in terms of the driving force (ΔG°), the reorganization energy (λ), and the electronic-coupling matrix element (H_{DA}), the last of which reflects the ET pathway.²⁴ Since these reactions involve PCET, the proton affinity is included in ΔG° and the structural changes that contribute to λ .²⁵

Density functional theory optimizations were performed on models (Scheme 1) of singly reduced and protonated NI and R sites to probe the thermodynamics and structural changes upon PCET (Scheme 2). The models included the second-sphere

Scheme 2. Computationally-Derived PCET Schematic for (A) NI and (B) R (See the SI for Details)



carboxylate (D72 in Lc),²⁶ as the equivalent of this residue has been shown to provide a critical negative charge in Fet3p (the MCO in yeast).^{10,27} The first electron into NI reduces the T3a Cu (the T3 Cu furthest from D72) and elongates the T3a Cu– μ_2 -OH bond. Protonation of this species is more favorable at the μ_3 -oxo by 16.8 kcal/mol relative to the T3 μ_2 -OH, resulting in a μ_2 -OH bridge between the oxidized T2 Cu and

T3b Cu, which are antiferromagnetically coupled. Protonation of the μ_2 -OH bridge of the one-electron-reduced R uncouples the T3 Cu ions, resulting in the reduction of the T3a Cu, the same Cu ion reduced in NI reduction.

Free energies for electron transfer [$\Delta G^\circ(e^-)$] and proton transfer [$\Delta G^\circ(H^+)$] were obtained with solvation corrections. From previous studies, there are four conserved second-sphere carboxylates near the TNC active site that neutralize its large positive charge (Figure S19).¹³ When negative point charges in the carboxylate positions were included, $\Delta G^\circ(e^-)$ increased and $\Delta G^\circ(H^+)$ decreased, but the sum of these free energies, $\Delta G^\circ(e^-+H^+)$, was not sensitive to the inclusion of these point charges (Table S3 in the SI). Therefore, the important comparison involves $\Delta G^\circ(e^-+H^+)$, which is approximately -7.0 kcal/mol more favorable for NI. Additionally, estimates for the inner-sphere reorganization energy λ as the difference in the energy of the starting geometry with an H-atom bound to the TNC and the energy of the optimized geometry for PCET were computed as 1.2 eV for NI and 1.5 eV for R.

The Marcus equation can be used to obtain an expression for the ratio of the two IET rates (eq S8 in the SI). Since the same Cu ion is reduced in both reactions, the values of H_{DA} are the same. From the known potentiometric electrochemical potential difference between the T1 and T3 sites in R ($\Delta G^\circ = -2.0$ kcal/mol),²⁸ it was found that with equivalent reorganization energies, the calculated $\Delta\Delta G^\circ(e^-+H^+)$ value of -7.0 kcal/mol gives a factor of $\sim 10^2$ difference in the IET rates (Table S4). The experimentally determined difference ($>10^3$) was obtained with a free energy difference of 10–12 kcal/mol or with $\Delta\Delta G^\circ(e^-+H^+) = -7.0$ kcal/mol and $\lambda_R \sim 0.3$ eV higher than λ_{NI} , consistent with above estimates (Tables S5 and S6). Thus, the difference in PCET driving force is the principal factor in determining the large difference in k_{IET} .

The molecular origin for the difference in PCET driving force in NI versus R is the structural difference of the two fully oxidized forms. In both PCET processes, the electron goes to T3a Cu, where the major structural difference between NI and R is the presence of the μ_3 -oxo ligand in NI. The strong donation of the μ_3 -oxo to T3a Cu results in a lower driving force for IET in NI compared with R, which would make IET to NI slower than that to R. However, since both IET reactions are PCET processes, the proton affinity contributes to the driving force, and the μ_3 -oxo in NI is a far stronger base than the T3 μ_2 -OH in R. The free energy difference in proton affinity for the μ_3 -oxo and μ_2 -OH in NI is 20.6 kcal/mol, which represents a ΔpK_a of ~ 15 between these basic ligands. Therefore, the large difference in ΔG° for IET to NI versus R is due to the μ_3 -oxo acting as a strong base to drive proton transfer.

This establishes that IET in NI reduction is fast, catalytically relevant, and due to the basicity of the μ_3 -oxo ligand. The μ_3 -oxo of NI originates from the reduction of O_2 and also provides the driving force for rapid enzyme rereduction. Therefore, in addition to being the four-electron oxidant, O_2 plays a critical role in enabling fast, catalytic rereduction of these oxidoreductases. This work has focused on the first electron in the reduction of NI. Two additional fast, catalytically relevant electron transfers are required to complete the catalytic cycle and are the focus of present research.

■ ASSOCIATED CONTENT**📄 Supporting Information**

Experimental and computational details and supporting data. This material is available free of charge via the Internet at <http://pubs.acs.org>.

■ AUTHOR INFORMATION**Corresponding Author**

edward.solomon@stanford.edu

Notes

The authors declare no competing financial interest.

■ ACKNOWLEDGMENTS

This research was supported by NIH Grant DK-31450 (E.I.S.).

■ REFERENCES

- (1) Solomon, E. I.; Sundaram, U. M.; Machonkin, T. E. *Chem. Rev.* **1996**, *96*, 2563.
- (2) Solomon, E. I.; Augustine, A. J.; Yoon, J. *Dalton Trans.* **2008**, 3921.
- (3) Solomon, E. I.; Szilagy, R. K.; DeBeer George, S.; Basumallick, L. *Chem. Rev.* **2004**, *104*, 419.
- (4) Solomon, E. I. *Inorg. Chem.* **2006**, *45*, 8012.
- (5) Allendorf, M. D.; Spira, D. J.; Solomon, E. I. *Proc. Natl. Acad. Sci. U.S.A.* **1985**, *82*, 3063.
- (6) Spira-Solomon, D. J.; Allendorf, M. D.; Solomon, E. I. *J. Am. Chem. Soc.* **1986**, *108*, 5318.
- (7) Gutteridge, J. M. C.; Stock, J. *Crit. Rev. Clin. Lab. Sci.* **1981**, *14*, 257.
- (8) Cracknell, J. A.; Vincent, K. A.; Armstrong, F. A. *Chem. Rev.* **2008**, *108*, 2439.
- (9) Mano, N.; Kim, H.-H.; Zhang, Y.; Heller, A. *J. Am. Chem. Soc.* **2002**, *124*, 6480.
- (10) Yoon, J.; Solomon, E. I. *J. Am. Chem. Soc.* **2007**, *129*, 13127.
- (11) Messerschmidt, A.; Rossi, A.; Ladenstein, R.; Huber, R.; Bolognesi, M.; Gatti, G.; Marchesini, A.; Petruzzelli, R.; Finazziagro, A. *J. Mol. Biol.* **1989**, *206*, 513.
- (12) Piontek, K.; Antorini, M.; Choinowski, T. *J. Biol. Chem.* **2002**, *277*, 37663.
- (13) Quintanar, L.; Yoon, J. J.; Aznar, C. P.; Palmer, A. E.; Andersson, K. K.; Britt, R. D.; Solomon, E. I. *J. Am. Chem. Soc.* **2005**, *127*, 13832.
- (14) Petersen, L. C.; Degn, H. *Biochim. Biophys. Acta* **1978**, *526*, 85.
- (15) Farver, O.; Wherland, S.; Koroleva, O.; Loginov, D. S.; Pecht, I. *FEBS J.* **2011**, *278*, 3463.
- (16) Huang, H. W.; Zoppellaro, G.; Sakurai, T. *J. Biol. Chem.* **1999**, *274*, 32718.
- (17) Cole, J. L.; Ballou, D. P.; Solomon, E. I. *J. Am. Chem. Soc.* **1991**, *113*, 8544.
- (18) Lee, S.-K.; DeBeer George, S. D.; Antholine, W. E.; Hedman, B.; Hodgson, K. O.; Solomon, E. I. *J. Am. Chem. Soc.* **2002**, *124*, 6180.
- (19) Andréasson, L. E.; Brändén, R.; Reinhammar, B. *Biochim. Biophys. Acta* **1976**, *438*, 370.
- (20) Warren, J. J.; Tronic, T. A.; Mayer, J. M. *Chem. Rev.* **2010**, *110*, 6961.
- (21) Westheimer, F. H. *Chem. Rev.* **1961**, *61*, 265.
- (22) Augustine, A. J.; Quintanar, L.; Stoj, C. S.; Kosman, D. J.; Solomon, E. I. *J. Am. Chem. Soc.* **2007**, *129*, 13118.
- (23) Gómez-Gallego, M.; Sierra, M. A. *Chem. Rev.* **2011**, *111*, 4857.
- (24) Marcus, R. A.; Sutin, N. *Biochim. Biophys. Acta* **1985**, *811*, 265.
- (25) Marcus theory is not a rigorous approach for PCET reactions but was employed here to determine the dominant factors that tune the kinetics of IET.
- (26) Nitta, K.; Kataoka, K.; Sakurai, T. *J. Inorg. Biochem.* **2002**, *91*, 125.
- (27) Quintanar, L.; Stoj, C.; Wang, T. P.; Kosman, D. J.; Solomon, E. I. *Biochemistry* **2005**, *44*, 6081.

(28) Reinhammar, B. R. M. *Biochim. Biophys. Acta.* **1972**, *275*, 245.